Electronic Supplementary Information

A facile approach to synthesize novel oxygen-doped g-C_3N_4 with superior visible-light photoreactivity

Jianghua Li, Biao Shen, Zhenhua Hong, Bizhou Lin, Bifen Gao and Yilin Chen*

Key Laboratory for Functional Materials of Fujian Higher Education, College of Materials Science and Engineering, Huaqiao University, Xiamen 361021, P. R. China.

Experimental Section

1. Materials

Dicyandiamide (98+%) and Hexachloroplatinic (IV) acid hexahydrate (99.95 %) were purchased from Alfa Aesar. Triethanolamine (AR) and hydrogen peroxide (30 vol.%) were purchased from Sinopharm Chem. Reagent Co. (Beijing, China). All reagents were used as received without further treatment.

2. Synthesis of g-C_3N_4 and O-doped g-C_3N_4

g-C_3N_4 was prepared by heating dicyandiamide at 550 ºC for 5 h under flowing high purity argon gas, followed by naturally cooling to room temperature under argon gas. The activation of g-C_3N_4 was undertaken by a H_2O_2 hydrothermal procedure. The g-C_3N_4 powder (0.6 g) was dispersed in 30 vol.% H_2O_2 solution (50 mL), and transferred into a Teflon-sealed autoclave, then maintained at 140 ºC for 10 h. The product was isolated by a centrifuge, and washed with water by five cycles of centrifugal separation/washing/redispersion. The final yield of the modified product was ca. 82 %.

3. Characterization

The morphology of the photocatalysts was characterized by a FEI XL-30 ESEM equipped with a

* *Corresponding author. Fax: +86-592-6162221; E-mail address: ylchen@hqu.edu.cn.*

field emission gun operating at 30 kV. The phase of the products was determined by XRD (Bruker D8 Advance). X-ray photoelectron spectroscopy (XPS) was recorded on an ESCALAB 250 photoelectron spectroscopy (Thermo Fisher Scientific Inc.) at 3.0×10^{-10} mbar with monochromatic Al *Kα* radiation (E = 1486.2 eV). The BET specific surface area and N_2 adsorption-desorption isotherms of samples were measured using a Quantochrome NOVA 1200e instrument at 77 K. The UV-vis DRS was performed with an UV-vis spectrometer equipped with an integrating sphere diffuse reflectance accessory (Shimadzu 2550). The PL spectrum was recorded on an Edinburgh FLS-920 spectrometer. Elemental analysis (EA) for nitrogen content in the sample was carried out on a Vario EL III CHN analyzer. The Fourier transform infrared spectra (FTIR) were recorded using a Thermo Scientific Nicolet iS10 FTIR spectrometer. Raman spectra were collected at room temperature using a micro-Raman spectrometer (Renishaw InVia) in the backscattering geometry with an Ar^+ laser (λ_{ex} = 785 nm).

4. Photocatalytic reactions

4.1 photocatalytic degradation of MB

The photocatalytic activities of the as-prepared samples were first evaluated via the photocatalytic degradation of MB in an aqueous solution under visible light irradiation. A 500 W halogen tungsten lamp (Philips, Q/YXKC33), which was positioned inside a cylindrical pyrex vessel surrounded by a circulating water jacket. An UV-cutoff filter (λ < 420 nm) was placed outside the jacket to ensure visible light illumination. To avoid photosensitization by MB, a $CuSO_4$ solution (200 $g\cdot L^{-1}$) was used to filter the light with wavelength beyond 600 nm. In each experiment, 80 mg of catalyst was mixed with a 80 mL MB solution (5 $mg\cdot L^{-1}$). Prior to irradiation, the suspension was magnetically stirred in the dark for 30 min to obtain a saturated MB absorption onto the catalyst. At irradiation time intervals of 20 min, the suspension (3 mL)

was collected, and separated by a centrifugal, then detected by a Shimadzu 2150 UV-Vis spectrometer.

4.2. Photocatalytic H_2 Production Activity

The photocatalytic H_2 evolution experiment was carried out in a top-irradiation vessel connected to a glass closed gas circulation and evacuation system at ambient temperature. As light source, a CEL-HXUV300 Xe arc lamp with a UV-cutoff filter ($\lambda < 420$ nm) was used. In the case of deposition of Pt, the loading of 1.2 wt.% Pt cocatalyst on the samples was performed by an in-situ photodeposition method. In a typical photocatalytic experiment, a total of 100 mg of the photocatalyst powder was suspended in 100 mL of aqueous solution containing 10 vol.% triethanolamine as sacrificial electron donor and equivalent molar amount of H_2PtCl_6 as co-catalyst. Before photocatalytic experiments, the reactant solution was evacuated for 40 min to remove air completely and to ensure the anaerobic conditions. The temperature of the reactant solution was maintained at 280 K by a flow of cooling water during the reaction. The amount of H_2 produced was analyzed with an online TCD gas chromatograph (GC 7890□, high purity argon as a carrier gas).

Fig. S1 shows the N_2 adsorption–desorption isotherms of the g-C_3N_4 and O-doped g-C_3N_4 samples. Both of the two samples are found to be of type IV isotherms with a hysteresis in the range of 0.45–0.99 P/P_0, which is characteristic for mesoporous materials.[1] The significant difference of N_2 adsorption volume between the g-C_3N_4 and the O-doped g-C_3N_4 reveals their different BET surface areas, which are 8.2 and 47 $m^2 \cdot g^{-1}$, respectively. Their corresponding pore diameter distributions calculated from BJH method are also exhibited. As shown, the sharp peak centered at 3.7 nm exists in both samples, which is probably attributed to layer-aggregated pores. Besides this, the extended wide peak at 5–15 nm in the O-doped g-C_3N_4 may be assigned to the pores corroded in the H_2O_2 hydrothermal process. It shows that the O-doped g-C_3N_4 benefits with larger BET surface area and extended pore diameter distribution from the O-doping. Such findings may contribute to the excellent catalytic activity observed on the doped sample.

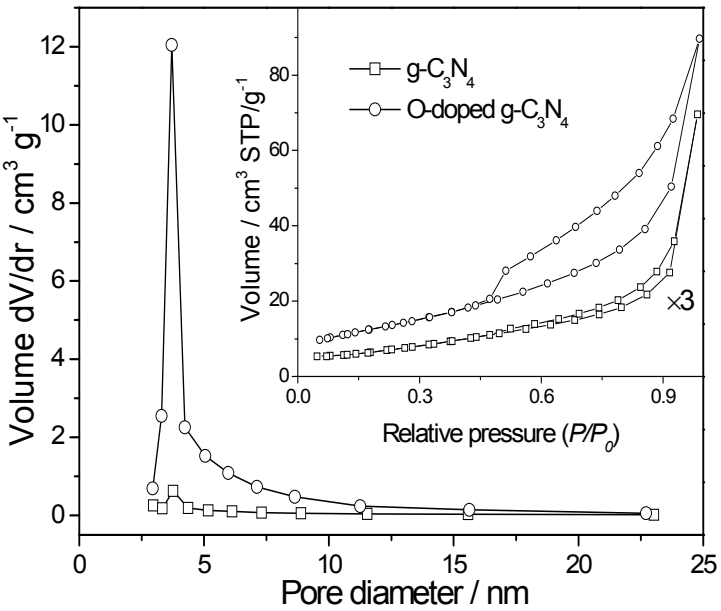

Fig. S1 The pore size distributions for the g-C_3N_4 and the O-doped g-C_3N_4. Insets: Nitrogen sorption isotherms at 77 K

Raman spectroscopy is a useful tool for studying crystalline quality because of its sensitivity to slight variations in the lattice symmetry.[2] So it is desirable to use Raman spectroscopy to confirm the presence of oxygen impurities in the O-doped C_3N_4 samples, as revealed by the XPS analysis. Fig. S2 shows a comparison of the Raman spectra among the g-C_3N_4 and the O-doped g-C_3N_4 used before and after. As shown, the g-C_3N_4 shows the characteristic peaks at 1100, 1138, 1199, 1217, and 1296 cm^{-1}.[3] All these characteristic bands can be also detected on the O-doped g-C_3N_4, suggesting no dramatic damage to the g-C_3N_4 skeleton after doping. Besides, the O-doped g-C_3N_4 exhibits two new Raman peaks at 1058 and 1118 cm^{-1}, which should be ascribed to the asymmetric vibration and the out-of-phase stretching vibration of C-O-C bond, respectively.[4,5] It suggests the oxygen impurities may substitute a faction of lattice nitrogen sites in the g-C_3N_4 matrix.

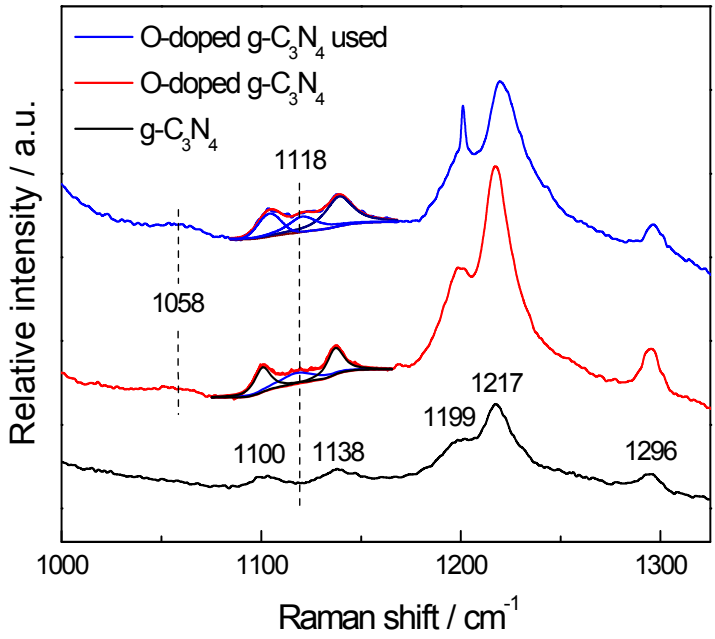

Fig. S2 Raman spectra of the g-C_3N_4 and the O-doped g-C_3N_4 used before and after the photocatalytic H_2 evolution experiment. The excitation time and power are 60 s and 1 mW, respectively.

IR and Raman spectroscopy are completely complementary, providing characteristic fundamental vibrations that are extensively used for the determination and identification of molecular structure. The FTIR spectra of the as-prepared samples are shown in Fig. 3S. Both the g-C_3N_4 and the O-doped g-C_3N_4 show the typical IR patterns of graphitic carbon nitride. The peaks in the region from 900 to 1800 cm^{-1} could be corresponding to the characteristic stretching modes of CN heterocycles.[6] According to the work of Larkin,[5] C-C, C-O, and C-N bonds have very similar force constants. Consequently, stretches involving C-C, C-O, and C-N strongly couple, giving rise to the skeletal stretching vibrations in the common IR regions. Liao *et al.* also reported that the peaks at ca. 1410 and 1060 cm^{-1} are ascribed to the C-O vibrations in C-OH and C-O-C functional groups, respectively.[7] Namely, the peaks of O-containing species in O-doped g-C_3N_4 might be located in the same region to trigonal C-N(-C)-C (full condensation) or bridging C-NH-C species. Moreover, because of the low quantity of oxygen atoms in the composites, it is difficult to definitely distinguish C-O species in the O-doped g-C_3N_4 by a FTIR spectrometer. However, note that the IR peaks at 1245 and 1413 cm^{-1} were respectively shifted by 9 and 8 cm^{-1} toward high frequencies after the O-doping (Fig. S3). The former could be attributed to the =C(sp^2) bending vibration while the latter should be ascribed to the out-of-phase stretching vibration of N-C(sp^3) bond.[5] It seems possible that the shifts might be caused by the electrophilic effect of the substitutional O atoms adjacent to C-N, resulting in the enhanced strength of C-N covalent bonds and the higher frequencies.

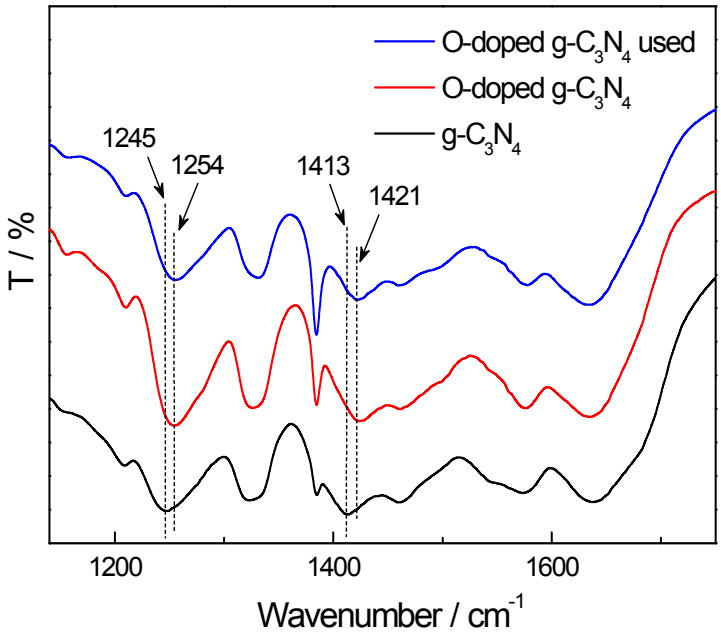

Fig. S3 FTIR spectra of the g-C_3N_4 and the O-doped g-C_3N_4 used before and after.

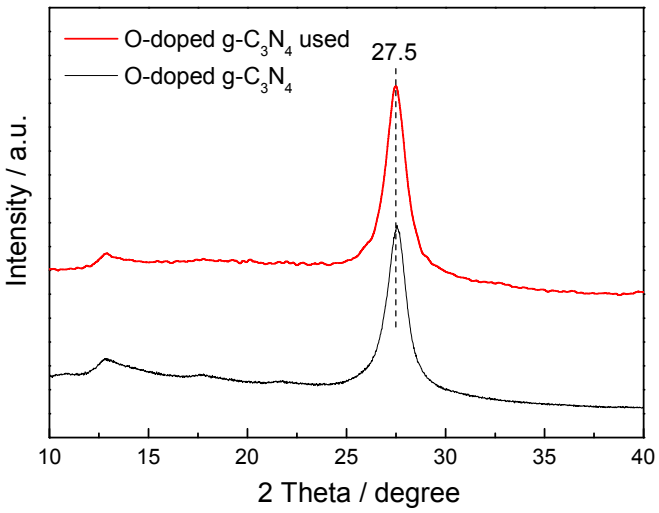

Fig. S4 XRD patterns of the O-doped g-C_3N_4 used before and after.

Tab. S1 XPS fitting data of the different samples

Sample	C 1s			N 1s			O 1s		
	Position (eV)	FWHM (eV)	Assignment	Position (eV)	FWHM (eV)	Assignment	Position (eV)	FWHM (eV)	Assignment
$g\text{-}C_3N_4$	284.6	1.38	C-C	398.5	1.38	$N(sp^2)$			
	286.1	1.50	$C\text{-}NH_2$	399.8	1.47	$N(sp^3)$	532.9	1.61	H_2O
	288.0	1.28	N-C-N	401.0	1.18	$C\text{-}NH_x$			
O-doped $g\text{-}C_3N_4$	284.6	1.42	C-C	398.5	1.44	$N(sp^2)$	531.6	2.30	N-C-O
	286.1	1.40	$C\text{-}NH_2$	399.8	1.45	$N(sp^3)$	532.8	1.53	H_2O
	288.0	1.35	N-C-N	401.0	1.45	$C\text{-}NH_x$	534.0	1.92	O_2 ads
	289.0	1.38	C-O						

Tab. S2 XPS N 1s spectra results of the $g\text{-}C_3N_4$ and the O-doped $g\text{-}C_3N_4$ samples

Sample	$N(sp^2)$	$N(sp^3)$	$C\text{-}NH_x$	$N(sp^2)/N(sp^3)$
$g\text{-}C_3N_4$	69.40%	23.13%	7.46%	3:1
O-doped $g\text{-}C_3N_4$	64.24%	24.76%	10.99%	2.6:1

Tab. S3 Atom concentration for C, N and O elements derived from the XPS spectra

Sample	C / at.%	N / at.%	O / at.%	C/N atomic ratio
g-C_3N_4	42.42	56.63	0.96	0.749
O-doped g-C_3N_4	39.46	52.56	7.98	0.751

Tab. S4 EA results of the g-C_3N_4 and the O-doped g-C_3N_4 samples

Sample	C / wt.%	N / wt.%	C/N atomic ratio
g-C_3N_4	37.61	58.71	0.747
O-doped g-C_3N_4	36.10	55.43	0.760

References

1 H. J. Yan, Y. Chen, S. M. Xu, *Int. J. Hydrogen Energ.*, 2012, **37**, 125–133.

2 P. V. Zinin, L. C. Ming, S. K. Sharma, V. N. Khabashesku, X. R. Liu, S. M. Hong, S. Endo, T. Acosta, *Chem. Phys. Lett.,* 2009, **472**, 69–73.

3 Q. J. Xiang, J. G. Yu, M. Jaroniec, *J. Phys. Chem. C.*, 2011, **115**, 7355–7363.

4 J. Rocks, L. Rintoul, F. Vohwinkel, G. George, *Polymer*, 2004, **45**, 6799–6811.

5 P. Larkin, *Infrared and Raman spectroscopy: principles and spectral interpretation*, Academic Press, Elsevier, 2011.

6 P. Niu, G. Liu, H. M. Cheng, *J. Phys. Chem. C.*, 2012, **116**, 11013−11018.

7 G. Z. Liao, S. Chen, X. Quan, H. T. Yu, H.M. Zhao, *J. Mater. Chem.*, 2012, **22**, 2721–2726.